Mem. S.A.It. Vol. 88, 551

Memorie della

Fragmentation of massive dense cores: the role of the magnetic field

F. Fontani[1], B. Commerçon[2], A. Giannetti[3], M.T. Beltrán[1], Á. Sánchez-Monge[4], and L. Testi[1,5]

[1] INAF-Osservatorio Astrofisico di Arcetri, Largo E. Fermi 5, I-50125, Florence, Italy
e-mail: fontani@arcetri.astro.it

[2] Ecole Normale Supérieure de Lyon, CRAL, UMR CNRS 5574, Université Lyon I, 46 Allée d'Italie, 69364, Lyon Cedex 07, France

[3] INAF-Istituto di Radioastronomia, via P. Gobetti 101, I-40129, Bologna, Italy

[4] I. Physikalisches Institut, Universität zu Köln, Zülpicher Str. 77, 50937 Köln, Germany

[5] European Southern Observatory, Karl-Schwarzschild-Str 2, D-85748, Garching bei München, Germany

Abstract. Massive stars and clusters are born of the gravitational collapse of massive, dense, gaseous clumps, and the way these systems form strongly depends on how the parent clump fragments into cores during collapse. Numerical simulations show that magnetic fields may be the key ingredient in regulating fragmentation. We have observed 11 massive and dense southern cores with the Atacama Large Millimeter Array (ALMA) in the thermal dust continuum emission at $\sim$ 1 mm with an angular resolution of $\sim 0.25''$, to determine their fragment population. In the first source studied in detail, IRAS 16061–5048c1, the ALMA image shows that the clump has fragmented into many cores along a filamentary structure. We find that the number, the total mass, and the spatial distribution of the fragments are consistent with fragmentation dominated by a strong magnetic field.

Key words. Stars: formation – ISM: clouds

1. Introduction

Massive and dense molecular cores ($M \geq 100$ $M_{\odot}$, and $n(H_2) \geq 10^4 cm^{-3}$) are believed to be the birthplaces of rich clusters and high-mass O-B stars. The formation of these systems starts from the fragmentation of the parent core occuring during its gravitational collapse, which is thus a crucial process in determining the final stellar population. In particular, the process has important implications in the theoretical debate of massive star formation ($M_* \geq$ 8 $M_{\odot}$), because the two main competing theories assume a totally different degree of initial fragmentation: in the core-accretion models (e.g. McKee & Tan 2003; Tan et al. 2013), massive stars are born from the direct collapse of a near-equilibrium core in which only one (or very few) fragments form; in the competitive accretion models (e.g. Bonnell et al. 2004), the parent core fragments into many low-mass seeds of the order of the thermal Jeans mass which competitively accrete from the common unbound gaseous envelope. Theoretical models and simulations show that the number, the size, the mass, and the spatial distribution of the fragments depend strongly on which of the main competitors of gravity is dominant. The main physical mechanisms that oppose gravity during collapse are: thermal pressure, intrinsic turbulence, protostellar feedback, and magnetic pressure (e.g. Hennebelle et al. 2011). However, at the beginning of the gravitational collapse, the thermal support is expected to be negligible, and the feedback from nascent protostellar objects through outflows, winds and/or expansion of ionised regions (especially from newly born massive objects) can be important only in relatively evolved stages (Bate 2009), but even then it seems to be of secondary importance (Palau et al. 2013). Therefore, the fragmentation at the earliest stages is influenced mainly by magnetic support and turbulence. In this respect, Commerçon et al. (2012) have shown that if the magnetic support dominates the dynamical evolution, only one or few fragments are expected, while many small fragments with mass of the order of $\sim 0.1 - 1$ $M_{\odot}$ separated by projected distances of $\sim 100 - 1000$ au are foreseen if the magnetic support is faint. Studies of the fragmentation level in massive clumps at the earliest stages of the gravitational collapse remain limited because pristine, massive clumps are rare, and typically located at distances larger than $\sim$ 1 kpc, hence reaching the linear resolution required for a consistent comparison with the simulations (about 1000 AU) requires observations with sub-arcsecond angular resolution. In this paper, we report on the population of fragments derived in the image of the dust thermal continuum emission at $\sim$ 278 GHz obtained with the Atacama Large Millimeter Array (ALMA) towards the source IRAS16061–5048c1, hereafter I16061c1, a massive ($M \sim 280 M_{\odot}$, Beltrán et al. 2006, Giannetti et al. 2013) and dense ($N(H_2) \sim 1.6 \times 10^{23}$cm^{-2}) molecular clump located at 3.6 kpc (Fontani et al. 2005).

2. Observations and results

Observations of I16061c1 with the ALMA array were performed during June, 2015. The array was in configuration C36-6, with maximum baseline of 1091 m. The phase centre was at R.A. (J2000): $16^h10^m06.''61$ and Dec (J2000): $-50°50'29''$. Details of the observations and data reduction procedures are given in Fontani et al. (2016). The angular resolution of the final image is $\sim 0.25''$ (i.e.$\sim$ 900 AU at the source distance). We were sensitive to point-like fragments of 0.06 $M_{\odot}$. The ALMA map of the dust thermal continuum emission is shown in Fig. 1(**B**): we have detected several dense condensations distributed in a filamentary-like structure extended east-west, surrounded by fainter extended emission. This structure has been decomposed into twelve fragments (Fig. 1(**B**)). The fragments were identified following these criteria: (1) peak intensity greater than five times the noise level; (2) two partially overlapping fragments are considered separately if they are separate at their half-peak intensity level. The main physical properties of the fragments derived from the continuum map, that is, integrated and peak flux, size, and gas mass, and the methods used to derive them, are described in Appendix A of Fontani et al. (2016).

3. Discussion and conclusions

We have simulated the gravitational collapse of I16061c1 through 3D numerical simulations following Commerçon et al. (2011), adopting a mass, temperature, average density, and level of turbulence of the parent clump very similar to those measured (Beltrán et al. 2006, Giannetti et al. 2013). In particular, the Mach number setting the initial turbulence was derived from the line width of $C^{18}O$ (3–2) by Fontani et al. (2012). Because these observations were obtained with angular resolution of $\sim 24''$, and the critical density of the line ($\sim 5 \times 10^4$cm^{-3}, Fontani et al. 2005) is comparable to the average density of the clump as a whole (Beltrán et al. 2006), the $C^{18}O$ line width represents a reasonable estimate of the intrinsic turbulence of the parent clump. The models were run for μ=2 (strongly magnetised case) and μ=200 (weakly magnetised case). Then, we post-processed the simulations data and computed the dust emission maps

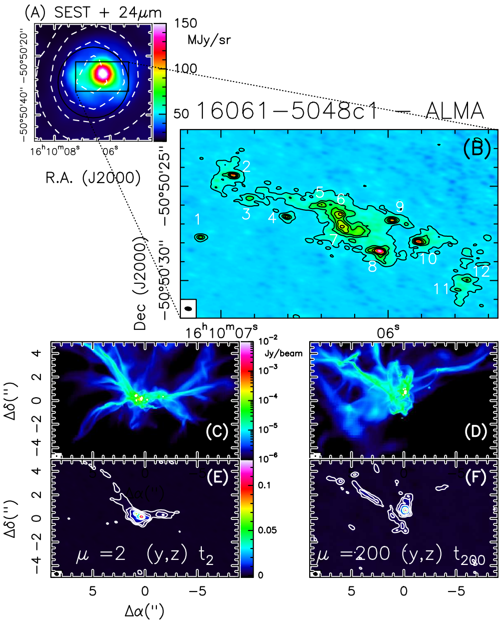

Fig. 1. **(A)**: Dust continuum emission map (dashed contours) obtained with the SEST telescope (angular resolution 24″) at 1.2 mm towards I16061c1 (Beltrán et al. 2006). The map is superimposed on the Spitzer-MIPS image at 24μm (units MJy/sr). **(B)**: Enlargement of the rectangular region indicated in panel **(A)**, showing the contour map of the thermal dust continuum emission at 278 GHz detected with ALMA (first contour and spacing = 0.54 mJy/beam). The ellipse in the bottom left corner shows the synthesized beam ($0.36 \times 0.18''$). The numbers indicate the twelve identified fragments (see Fontani et al. 2016) **(C)**: Simulations of the thermal dust emission at 278 GHz predicted by the models of Commerçon et al. (2011), which reproduce the gravitational collapse of a 300 $M_\odot$ clump in case of strong magnetic support (μ = 2), obtained at time t_2 (see Fontani et al. 2016), projected on a plane perpendicular to the direction of the magnetic field. **(D)**: Same as panel **(C)** for the case μ = 200 and time t_{200} (see Fontani et al. 2016). **(E)**: Synthetic ALMA images of the models presented in panel **(C)**. The contours correspond to 0.54, 1.2, 2, 5, 10, 30, and 50 mJy/beam. **(F)**: same as panel (E) for the case μ = 200 (weak magnetic support).

at 278 GHz (Fig. 1 C–F): the final maps obtained in flux density units at the distance of the source were imaged with the CASA software to reproduce synthetic images with the same observational parameters as those of the observations. Based on the overall morphologies shown in Fig. 1 and on the statistical properties of the fragments reported in Fontani et al. (2016), the model that better reproduces the data clearly is the one with μ=2. Hence, with these new ALMA observations, compared with realistic 3D simulations that assume as initial conditions the properties of the parent clump, we demonstrate that the fragmentation due to self-gravity is dominated by the magnetic support, based on the evidence that (1) the overall morphology of the fragmenting region is filamentary, and this is predicted only in case of a dominant magnetic support; (2) the observed physical parameters of the fragments are better reproduces by simulations assuming substantial magnetic support.

References

Bate, M.R. 2009, MNRAS, 392, 1363

Beltrán, M.T., Brand, J., Cesaroni, R., et al. 2006, A&A, 447, 221

Bonnell, I.A., Vine, S.G., Bate, M.R. 2004, MNRAS, 349, 735

Commerçon, B., Hennebelle, P., Henning, T. 2011, ApJ, 742, L9

Commerçon, B., et al. 2012, A&A, 545, 98

Fontani, F., et al. 2005, A&A, 432, 921

Fontani, F., Giannetti, A., Beltrán, M.T., et al. 2012, MNRAS, 423, 2342

Fontani, F., Commerçon, B., Giannetti, A., et al. 2016, A&A, 593, L14

Giannetti, A., et al. 2013, A&A, 556, 16

Hennebelle, P., Commerçon, B., Joos, M., et al. 2011, A&A, 528, 72

McKee, C. & Tan, J.C. 2003, ApJ, 585, 850

Palau, A., Fuente, A., Girart, J.M., et al. 2013, ApJ, 762, 120

Sanchez-Monge, Á, Beltrán, M.T., Cesaroni, R., et al. 2013, A&A, 550, 21

Tan, J.C., et al. 2013, ApJ, 779, 96